Experimental evaluation of the magnetization process in a high T_c bulk superconducting magnet using magnetic resonance imaging

Daiki Tamada*[1, 2], Takashi Nakamura[1, 2], Yoshitaka Itoh[3], Katsumi Kose[1]

1. Institute of Applied Physics, University of Tsukuba, Tsukuba 305-8573, Japan
2. RIKEN, Wako, 351-0198, Japan
3. IMRA Material R&D Co., Ltd., Kariya, 448-0021, Japan

* Electric mail: tamada@mrlab.frsc.tsukuba.ac.jp

Abstract

We measured the magnetic field distribution of a high T_c bulk superconducting magnet (c-axis oriented $EuBa_2Cu_3O_y$ crystals) during the magnetization process using magnetic resonance imaging. Measurements were performed in the field cooling process from 100 to 50 K in a 4.74 T magnetic field and in the field reducing process from 4.74 to 0 T at 50 K. In field cooling, we observed a significant decrease in the gradient coil efficiencies caused by the Meissner effect. Analysis of the trapped field suggested the presence of temperature gradients, microcracks, and inhomogeneity in the bulk crystals.

1. Introduction

A high critical temperature (T_c) superconducting (HTS) bulk magnet is a novel magnet for nuclear magnetic resonance (NMR) and magnetic resonance imaging (MRI) [1, 2]. The bulk magnet acts like a permanent magnet by trapping an external magnetic field and can produce a strong (up to about 17 T) [3] and stable magnetic field like a conventional superconducting magnet (SCM) without a large installation space, because the cryostat structure is very simple.

In 2007, Nakamura et al. reported a bulk magnet using annular bulk superconductors (Sm-Ba-Cu-O) energized at 3T and achieved magnetic field homogeneity of 2400 ppm (peak-to-peak: PP) in the ϕ1.2 mm × 5.0 mm cylindrical region [1]. They observed the first NMR spectrum of ^{1}H using the bulk superconducting magnet. In 2010, Ogawa et al. developed the first MRI system using an HTS bulk magnet made of c-axis oriented single-domain Eu-Ba-Cu-O crystals [2, 4]. They achieved magnetic field homogeneity of 37 ppm PP with first order shimming, which is performed by adjusting the offset current for the three axes gradient coil, in the ϕ6.2 mm × 9.1 mm cylindrical region and acquired a clear three dimensional (3D) MR image of a chemically fixed mouse fetus. Although they succeeded in the first NMR and MRI experiments using the bulk superconducting magnets, we have found that the magnetic field distribution of the bulk magnet is not reproducible and depends on its magnetization process.

In this study, we quantitatively evaluated the magnetization process of the bulk magnet by measuring its 3D magnetic field distribution using an MRI based method to obtain information that would be useful for developments of high-quality bulk superconducting magnets.

2. Material and methods

The MRI system we used consists of a superconducting bulk magnet, a 3-axis gradient coil set, an 8 mm diameter saddle shaped RF coil, and an MRI console as shown in Fig. 1. The bulk

magnet comprised six annular superconductors (60 mm outer diameter (OD), 28 mm inner diameter (ID), 20 mm high, T_c = 93K) made of c-axis oriented single-domain $EuBa_2Cu_3Oy$ crystals containing 20 wt. % Ag [5]. The bulk superconductors were reinforced with 5 mm-thick aluminum rings to protect them from the cracking [6, 7] caused by the huge electromagnetic hoop stress.

The bulk magnet was installed in a cryostat with a room temperature (RT) bore diameter of 23 mm. The bulk magnet was cooled with a pulse tube refrigerator through the cold head placed in the vacuum chamber of the cryostat. The temperature T_b of the bulk magnet was monitored and controlled using a Pt resistor sensor and an electric heater attached to the cold head.

The gradient coil set was wound on an acrylic pipe with OD of 16.8 mm and an ID of 14.8 mm using a 0.3 mm diameter polyurethane-coated Cu wire. The axial gradient coil was a Maxwell pair coil and the transverse gradient coils were Golay coils. The efficiencies of the Gx, Gy, and Gz coils were 81 mT/m/A, 93 mT/m/A, and 106 mT/ m/A, respectively. The radio frequency (RF) coil was a single-turn saddle shaped coil wound on an acrylic pipe with 12 mm OD and 9 mm ID using 0.1 mm-thick Cu foil. The RF probe was tuned to 202.0 MHz using two variable capacitors and one fixed. The gradient set and the RF probe were inserted into the RT bore of the bulk magnet and connected to the MRI console (MRTechnology, Tsukuba, Japan).

The bulk magnet was magnetized by a field cooling method to achieve a homogeneous magnetic field for NMR/MRI as follows.

First, the bulk magnet was cooled down to 100 K using the refrigerator in a constant external magnetic field B_e (field strength = 4.74 T, proton resonance frequency = 202.17 MHz) produced by a conventional SCM (JRTC-300/89, JASTEC, Kobe, Japan). Then, B_e was homogenized by using superconducting shimming. After the temperature of the bulk magnet stabilized, the bulk magnet was cooled down to 50 K while the spatial distribution of the magnetic field B_z of the bulk magnet was measured at temperatures of 100, 93, 84, 70, 60, and 50

K. Then, B_e was reduced down to 0 T at the rate of 24 mT per minute while the spatial distribution of B_z was measured at B_e of 4.74, 4.0, 3.0, 2.0, 1.0, and 0 T. Finally, the bulk magnet was removed from the RT bore of the conventional superconducting magnet carefully after being cooled down to 40 K to stabilize the trapped magnetic flux.

The spatial distribution of B_z was measured using $CuSO_4$-doped water in an 8 mm diameter NMR sample tube and a phase-shift method based on 3D spin echo imaging sequences (TR/TE = 100 ms/20 ms, field of view = 12.8 mm^3, matrix size = 64^3). The homogeneity of B_z was evaluated in the central ϕ6 mm × 6 mm cylindrical area. The spatial distribution of B_z was approximated by a linear combination of spherical harmonic functions T_{nm} up to the second order as

$$B_z = \sum_{n=0}^{2} \sum_{m=-n}^{n} H_{nm} T_{nm} \quad , \tag{1}$$

$$T_{nm} = \begin{cases} \frac{1}{\sqrt{2}}(Y_{nm} + Y_{n-m}) & (m > 0) \\ \frac{1}{\sqrt{2i}}(Y_{nm} - Y_{n-m}) & (m < 0) \\ Y_{nm} & (m = 0) \end{cases}, \tag{2}$$

$$Y_{nm} = r^n P_{nm}(\cos\theta)\cos[m(\varphi - \sigma_{nm})], \tag{3}$$

where n is order, m is degree, P_{nm} is the associated Legendre function, and σ_{nm} is the phase corresponding to n and m in polar coordinate (r, θ, ϕ).

The efficiencies of the gradient coils, defined by the gradient field strength per unit current, were calculated using the numbers of pixels for the length (along z) and diameters (along x and y) of the $CuSO_4$ doped water of the 3D spin echo images.

3. Results and Discussion

Figure 2 shows the inhomogeneity in B_z and the resonance frequency (MHz) plotted against the temperature T_b of the bulk magnet during the cooling process. The inhomogeneity

varied around 10 ppm, and this variation was not reproducible among repeated experiments. On the other hand, the resonance frequency increased with decreasing T_b, and this variation was reproducible among repeated experiments. At present, the origin of the resonance frequency increase is unknown.

Figure 3 shows MR images acquired using an identical pulse sequence at T_b of 100 and 70 K, which demonstrated that efficiencies of the gradient coils decreased when the bulk magnet was cooled down to below T_c. Figure 4 shows efficiencies of the gradient coils plotted against T_b, clearly showing that the magnetic field gradients were reduced by the shielding currents induced in the bulk superconducting material because the magnetic flux generated by the gradient coils was expelled according to the Meissner effect. To our knowledge, this phenomenon is the first observation for gradient coils used in MRI. In order to avoid this undesirable effect, shield coils [8], which eliminate the magnetic field outside gradient coils, will be required.

Figure 5 shows the inhomogeneity of B_z and the resonance frequency (MHz) plotted against the external magnetic field B_e. The proton resonance frequency of the bulk magnet slightly decreased with decreasing B_e, and finally became almost equal to the initial value of the conventional superconducting magnet. The inhomogeneity of B_z linearly increased.

Figure 6 shows the three dimensional B_z distribution measured at B_e for (a) 4.74, (b) 4.0, (c) 3.0, (d) 2.0, (e) 1.0, and (f) 0 T in the field reducing process. It is clear from this figure that the homogeneity degraded significantly around the bottom of the cylindrical area in the field trapping process with decreasing B_e.

Figure 7 shows the magnitude of the magnetic field components corresponding to T_{nm}. The magnitude of the component was defined as the PP value of the spatial function corresponding to the component. The components corresponding to T_{1-1}, T_{10}, T_{21}, and T_{2-1} varied considerably with decreasing B_e, although variations of other components were not significant. Higher-order components, such as third- and fourth-order components, were not significant because the root mean square error of the measured distribution was less than 3 ppm.

Several origins were considered for the inhomogeneity of the trapped magnetic field.

The first is the inhomogeneous temperature distribution of the bulk magnet. As described in the previous section, the bulk magnet was cooled with the cold head located just below the magnet and the bulk magnet is long (120 mm) in the vertical direction. Therefore, the vertical temperature gradient cannot be neglected, which may affect the magnetic field trapping property of the bulk magnet [9, 10] and produce vertical components of the inhomogeneityIt is essential to improve thermal conductivity by using a sophisticated cooling technique such as the alloy impregnation [3].

The second is the presence of microcracks in the bulk material. When we repeated the field cooling experiments several times, we observed some irreversible or unrecoverable degradation in the homogeneity of the trapped magnetic field. Therefore, we considered that this degradation may be attributed to some irreversible damage of the bulk crystals because the bulk material was subject to very huge hoop stress in the large magnetic field. In regard to this, decreasing the reducing rate of B_e is one of the solutions although it consume more process time.

The third is inhomogeneity in the bulk material itself. The bulk crystals were carefully grown in a furnace for several months to achieve uniform property over the crystals. However, some uncontrollable conditions (*e.g.* gravity) may produce some variations among or over the crystals. The variations among the bulk crystals may be confirmed by changing the relative location of the crystals and repeating the field cooling experiments, but possible damage of the crystals may make this difficult.

The fourth is the limitation of the computer simulation used to design the bulk material. The odd-order (1st, 3rd, …) inhomogeneity along the z direction was not caused by the limitation of the computer simulation; however, the even-order (2nd, 4th, …) inhomogeneity along the z direction might have been caused by insufficiency of the computer simulation.

At present, we could not identify the origin of the inhomogeneity of the trapped magnetic field. However, because we have developed a very powerful method of measuring the magnetic

field distribution of the bulk magnet, we believe that a more homogeneous magnetic field will be obtained in future.

4. Conclusions

In this study, we measured the magnetic field distribution in a bulk magnet in both the field cooling process in the constant external magnetic field (4.74 T) and in the reducing external field in the constant temperature (50 K). In the field-cooling experiments, we observed for the first time a significant decrease (~30%) of the efficiencies of the gradient coils caused by the Meissner effect. The trapped magnetic field was analyzed using spatial harmonic functions, which gave us useful information about the origins of the field inhomogeneity. In conclusion, our experimental results and a future computer simulation for the bulk magnet will develop a new instrumental design, a new magnetization protocol, and a new bulk magnet design to achieve a more homogeneous magnetic field for NMR and MRI.

Acknowledgements

We acknowledge Drs T. Haishi at MRTechnology and Y. Terada at University of Tsukuba for useful comments on the manuscript.

References

[1] T. Nakamura, M. Yoshikawa, Y. Itoh, H. Koshino, *Concept Magn. Reson. B (Magn. Reson. Eng.)* **31B (**2007**)** 65.

[2] K. Ogawa, T. Nakamura, Y. Terada, K. Kose, T. Haishi, *Appl. Phys. Lett.* **98 (**2011**)** 234101.

[3] M. Tomita, M. Murakami, *Nature* **421 (**2003**)** 517

[4] T. Nakamura, Y. Itoh, M. Yoshioka, N. Sakai, S. Nariki, I. Hirabayashi, H. Utsumi, *TEION KOGAKU* **48 (**2011**)** 139 (in Japanese)

[5] F. Yeh, K. W. White, *J. Appl. Phys.* **70 (**1991**)** 4989

[6] P. Diko, *Mat. Sci. Eng.* **B53 (**1998**)** 149

[7] T. H. Johansen, *Phys. Rev. B* **60 (**1999**)** 9690

[8] R. Turner, *Magn. Reson. Med*, **11**(1993)903

[9] M. Sawamura, M. Morita, H. Hirano, *Physica C* **531 (**2003**)** 392

[10] S. Nariki, N. Sakai, M. Matsui, M. Murakami, *Physica C* **774 (**2002**)** 378

Figure captions

FIG. 1. The MRI system consisting of an MRI console and a superconducting bulk magnet. A 3-axis gradient coil set and an 8 mm diameter saddle shaped RF were inserted in the RT bore of the bulk magnet. An 8 mm diameter NMR sample tube with $CuSO_4$-doped water was set in the RF coil.

FIG. 2. Inhomogeneity of the B_z (PP) and the resonance frequency (MHz) plotted against T_b during the cooling process.

FIG. 3. MR images of $CuSO_4$-doped water in an NMR sample tube acquired using a 3D spin echo sequence at T_b of (a) 100, and (b) 70 K, respectively.

FIG. 4. Efficiencies of the gradient coils plotted against T_b during the cooling process.

FIG. 5. Inhomogeneity of the B_z (PP) and resonance frequency (MHz) plotted against the external magnetic field B_e.

FIG. 6. Spatial distribution of B_z at Be of (a) 4.74, (b) 4.0, (c) 3.0, (d) 2.0, (e) 1.0, and (f) 0 T.

FIG. 7. Magnitude of the magnetic field components corresponding to T_{nm} plotted against B_e.

Figures

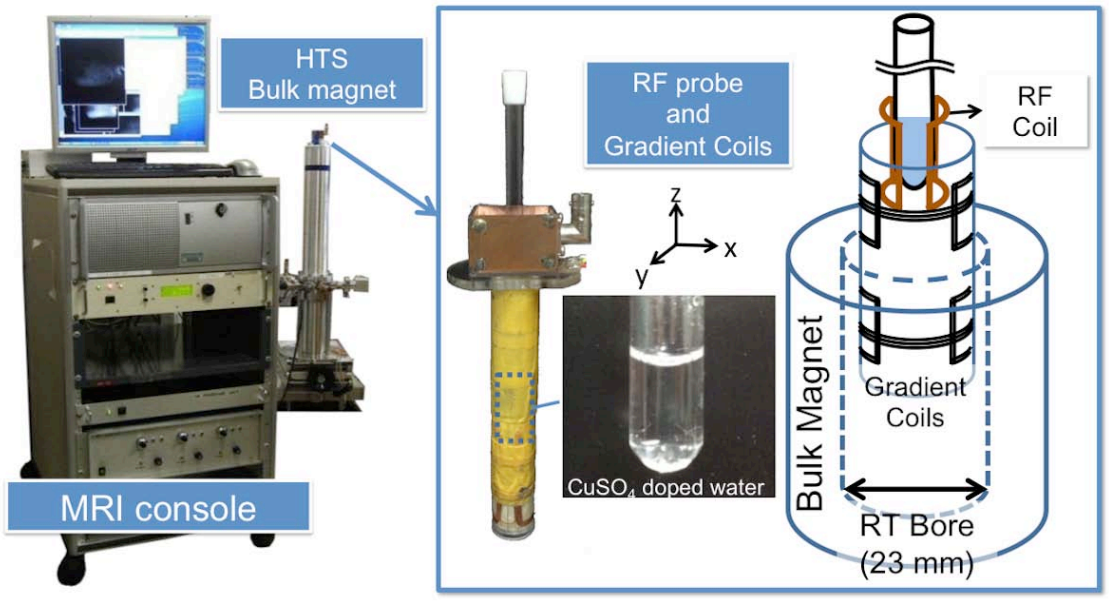

FIG. 1. The MRI system consisting of an MRI console and a superconducting bulk magnet. A 3-axis gradient coil set and an 8 mm diameter saddle shaped RF were inserted in the RT bore of the bulk magnet. An 8 mm diameter NMR sample tube with CuSO4-doped water was set in the RF coil.

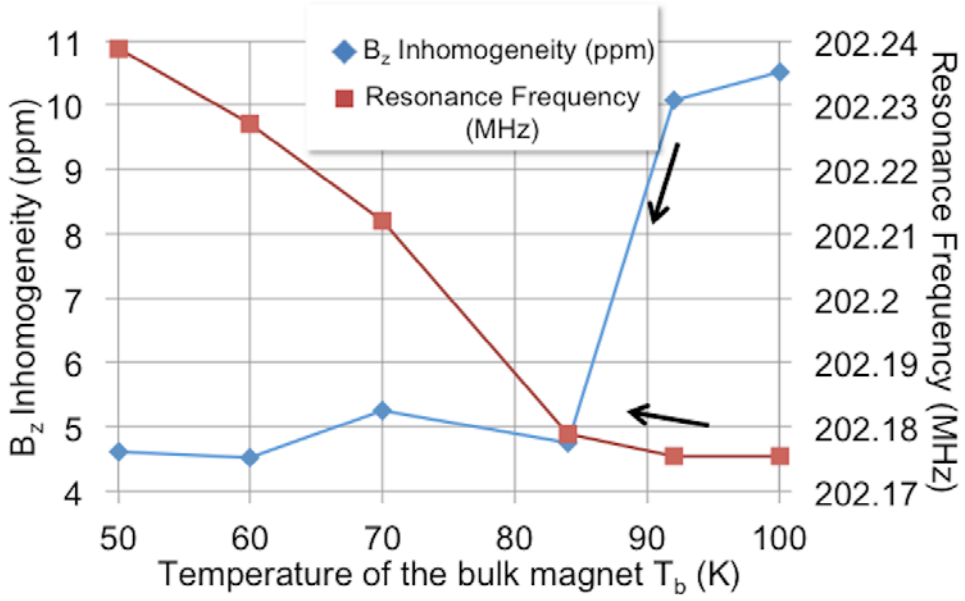

FIG. 2. Inhomogeneity of the B_z (PP) and the resonance frequency (MHz) plotted against T_b during the cooling process.

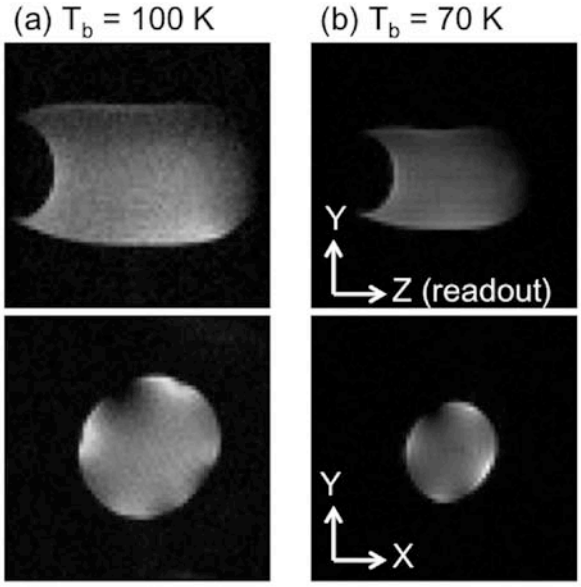

FIG. 3. MR images of $CuSO_4$-doped water in an NMR sample tube acquired using a 3D spin echo sequence at T_b of (a) 100, and (b) 70 K, respectively.

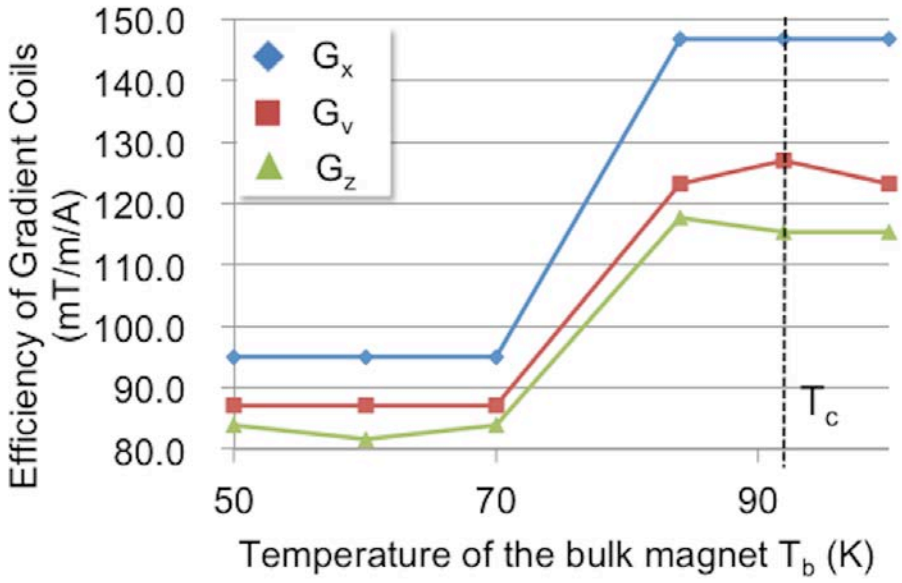

FIG. 4. Efficiencies of the gradient coils plotted against T_b during the cooling process.

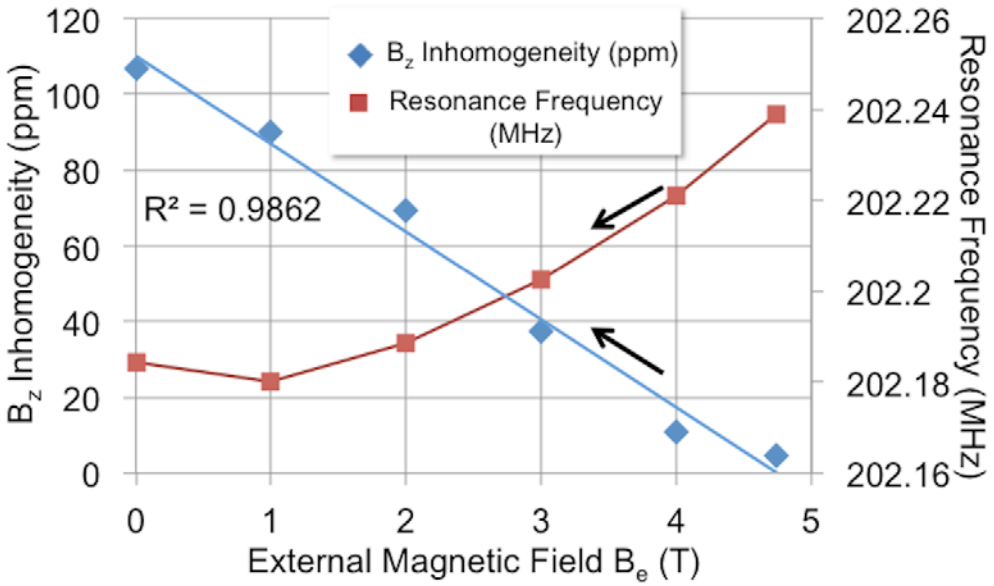

FIG. 5. Inhomogeneity of the B_z (PP) and resonance frequency (MHz) plotted against the external magnetic field B_e.

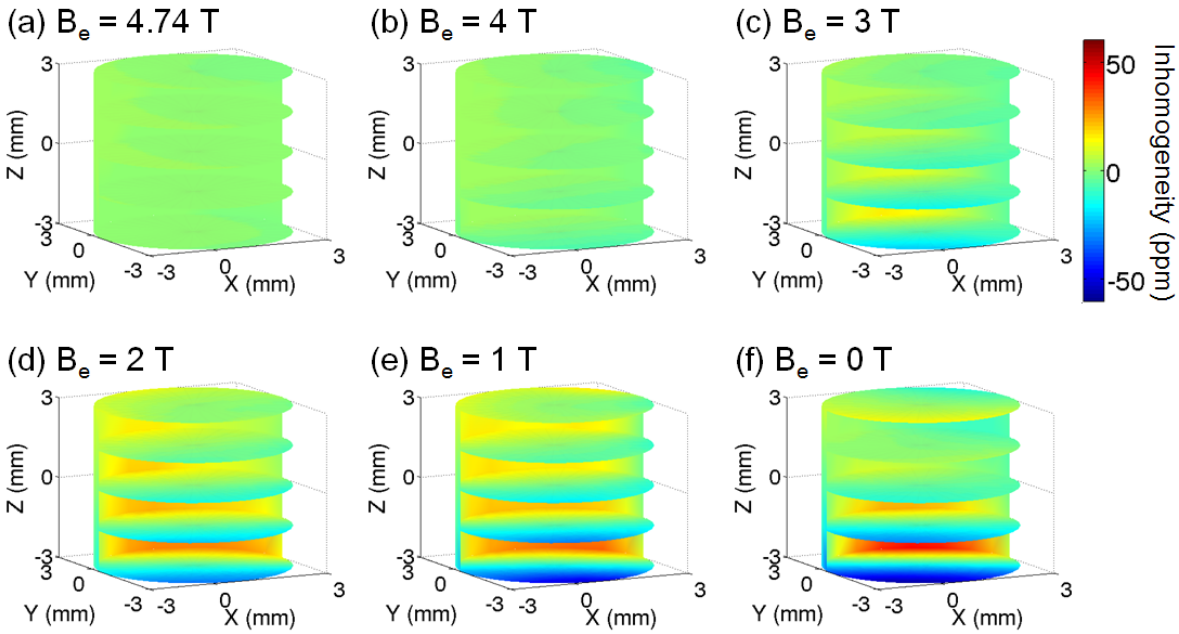

FIG. 6. Spatial distribution of B_z at Be of (a) 4.74, (b) 4.0, (c) 3.0, (d) 2.0, (e) 1.0, and (f) 0 T.

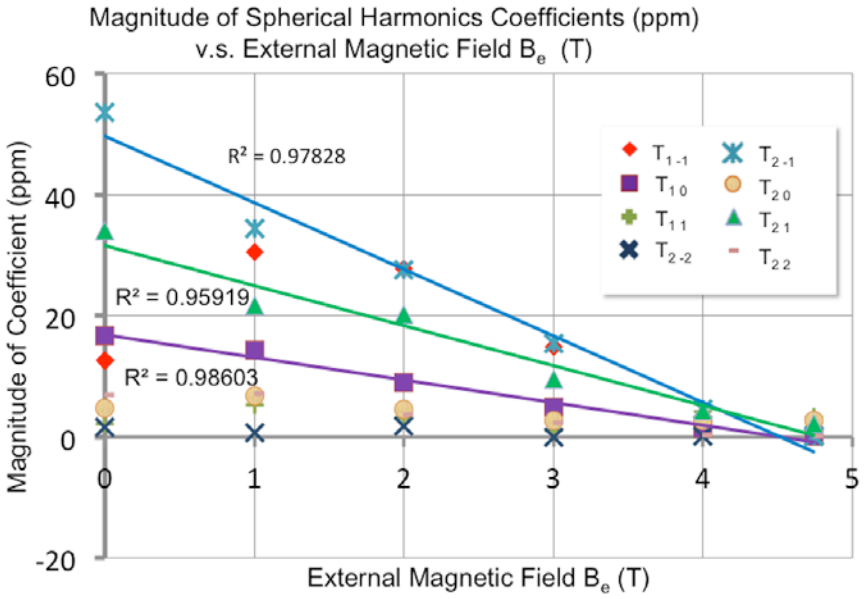

FIG. 7. Magnitude of the magnetic field components corresponding to T_{nm} plotted against B_e.